Surface Coil Techniques for In Vivo NMR

M. Robin Bendall*

School of Science
Griffith University
Nathan, Queensland
Australia 4111

(* On leave in the Department of Applied Sciences in Medicine, University of Alberta, Edmonton, Canada.)

I. INTRODUCTION

The application of nuclear magnetic resonance to the study of live animal and human subjects is a rapidly growing field of interest of established importance for biochemical and clinical studies. NMR imaging is now a routine modality in many clinical settings and *in vivo* NMR spectroscopy is a widely-accepted research method. Imaging is normally restricted to the detection of the abundant and NMR-sensitive ^{1}H nuclei of water and fat, and commonly, circumscribing r.f. coils which surround the head or body are used for r.f. irradiation and detection of the NMR signals. Generally, circumscribing coils do not have sufficient sensitivity to detect other ^{1}H containing metabolites, or other magnetically active nuclei, in localized regions of a human or animal, and almost all *in vivo* spectrocopic studies have utilized surface coils placed close to the region of interest. Surface coils of various types will probably remain the major tool of the *in vivo* spectroscopist. In the short term it is reasonable to invest considerable research effort in their development which is the most promising means of expanding routine clinical applications.

This review is addressed entirely to surface coil techniques, especially pulse sequences useful for optimization of signal-to-noise, localization and spectral simplification. The already myriad of application papers, especially utilizing ^{31}P NMR, are not discussed.

Maximum sensitivity is of paramount importance in *in vivo* spectroscopy. A small flat surface coil, placed on the surface of an animal or human subject, is the most sensitive way of obtaining spectra from tissues close to the surface and, in consequence, most physiological data from intact animals or humans have been obtained in this way. Optimization of signal in the presence of the spatially varying r.f. field of the surface coil is discussed briefly in section IV, and considered further in relation to methods discussed in later sections.

The variation of sensitivity throughout the sample is directly related to the spatial variation of the r.f. field produced by the surface coil. This property of r.f. inhomogeneity displayed by all surface-type coils must be taken into account for any sequence of r.f. pulses applied with the coil. The problem can be simplified, since most useful pulse sequences can be broken down into the well-known inversion-recovery or spin-echo sequences, and such an analysis is used below to describe various localization methods, as well as methods for simplifying or editing *in vivo* NMR spectra. The simple phase cycling schemes required for inversion-recovery or spin-echo sequences when using surface coils are described in section II.

The rapid decrease of the sensitivity of the surface coil to regions at increasing distance from the coil provides a crude form of sample localization. However, the sensitive volume does not have hard boundaries and its detailed shape

(discussed in section III) is quite complex and dependent on the experimental variables selected. It is always dangerous to assume that this crude localization is sufficient, though it may be in some cases, and many published studies which have ignored this problem are questionable. A common problem is the intense signals from the intervening tissue between the surface coil and the tissue of interest. For example, surface coil ^{31}P spectra of the brain will include extracranial muscle and scalp tissue. Conversely ^{1}H NMR showing lactate in abnormal brain tissue would probably not be compromised by ^{1}H signals from the scalp. The reverse situation applies to the human limbs, where ^{1}H lactate signals from within ischaemic muscle would be swamped by lipid signals from the intervening fat layer, but the fat layer produces no significant ^{31}P signals to invalidate the ^{31}P spectrum. For the liver, the intervening muscle wall and fat layer would compromise both the ^{31}P and the ^{1}H spectrum respectively. Another common problem is the diffuse boundary of the sensitive volume which may for example extend into non-exercised muscle in the case of human limb studies, or into normal brain tissue in the case of surface brain tumor or stroke investigations. Clearly, in general, additional means of sensitive-volume localization are required so that it can be stated with certainty that say 80 to 90% of the signal for a particular metabolite originates from the region of interest. Such a criterion could be relaxed if changes in the level of a particular metabolite were measured in a set of routine experiments and if it were known that such changes were only occurring in the tissue of interest, but this would have to be proven by complete localization prior to the set of routine experiments.

The major part of this review is devoted to additional techniques for localizing the sensitive volume. These fall into two main classes: methods which require magnetic field gradients (section V) and methods which utilize r.f. inhomogeneity (section VI). A third class combines these two methods (section VII) and a fourth class uses multiple r.f. coils, one of which will be a surface coil (section VIII). Throughout, most emphasis will be placed on surface-type coils, but the generalization of some methods to three-dimensional localization as might also be appropriate for a circumscribing coil will also be discussed.

In traditional NMR spectroscopy, the simplification of spectra by relaying information between two J-coupled nuclei has been a very important area of research for the last decade. There are also important applications in *in vivo* spectroscopy and this is explored in sections IX and X.

II. INVERSION-RECOVERY AND SPIN-ECHO SEQUENCES IN INHOMOGENEOUS R.F. FIELDS

For a homogeneous r.f. coil the inversion-recovery and spin-echo pulse sequences may be written respectively as

$$180^\circ - \tau - 90^\circ \text{ ; acquire signal,} \qquad (1)$$

and $$90^\circ - \tau - 180^\circ - \tau - \text{acquire,} \qquad (2)$$

where τ is a delay period between the pulses. For inhomogeneous r.f. coils such as surface coils, the 180° and 90° pulses have little meaning because pulse angles vary continuously and rapidly through-out sample space, and variable 2θ and θ pulses are appropriate. When θ differs markedly from 90°, intense anomolous signals arise, and it has been widely believed that these sequences cannot be used with a surface coil (1-3). However, it has been shown using simple vector diagrams (4,5) or rotation matrices (6), that these artifacts can be entirely eliminated for any value of θ by suitable phase cycling of the pulses during a series of transients, which for sequences (1) and (2) respectively is

$$2\theta[\pm x] - \tau - \theta\text{; acquire,} \qquad (3)$$

and

$$\theta - \tau - 2\theta[\pm x,\pm y] - \tau - \text{acquire, receiver}[+,-] \qquad (4)$$

The phase-cycled inversion pulse, $2\theta[\pm x]$, signifies that the pulse phase is alternated between +x and -x for alternate transients, and this is a more general variation (5-8) of the method introduced by Demco et al (9) and initially used with surface

coils (4,10,11). The phase cycling of the 2θ[±x,±y] refocusing pulse is as introduced by Bodenhausen et al (12) for two-dimensional high-resolution NMR, and receiver [+,-] means that the receiver phase is inverted (i.e. the signal is subtracted) when the 2θ pulse is cycled through the ±y phases.

We have shown (5,6) that the three types of pulses in sequences (3) and (4) are basic building blocks of surface-coil sequences. Each sequence must have one excitation pulse θ, but depending on the purpose of the sequence, any number of 2θ[±x] or 2θ[±x,±y] type pulses may be used (provided the phase cycling for each pulse is independent of all others), with or without τ delays.

To quantify the effect of these variable r.f. pulses, abstract mathematics can be used (6) or a better physical feel for the various pulse sequences may be obtained using vector diagrams (4,5). For example, Figure 1a shows the effect of a variable θ pulse on initial z magnetization. Thus it can be readily shown that a 2θ[±x] pulse before the θ excitation pulse reduces initial z magnetization to an amount given by cos2θ. The θ pulse converts unit z magnetization to detectable transverse (xy) magnetization equal to sinθ (as shown in Figure 1a), and a 2θ[±x,±y] pulse reduces the latter to an amount given by $\sin^2\theta$. For multiple pulse sequences, these various trigonometric factors are multiplied together: eg. if two 2θ[±x] pulses were used prior to θ and one 2θ(±x,±y] pulse after θ, signal intensity would be proportional to $\cos^2 2\theta \sin^3\theta$.

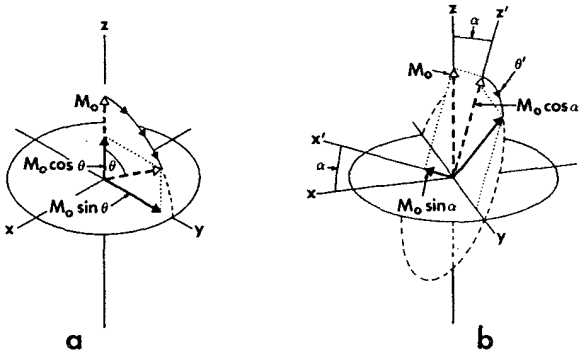

Figure1. (a) An r.f. pulse of angle (or length) θ and of x phase rotates an initial z magnetization M_0 through an angle θ about the x axis of the rotating reference frame and generates a detectable transverse component of y phase (absorption-mode) proportional to sinθ. (b) The same pulse applied off resonance rotates M_0about the tilted x' axis. This rotation is equivalent to the resultant of a stationary component $M_0 \sin\alpha$ and rotation of $M_0 \cos\alpha$ in the tilted yz plane. The final y component is $M_0 \cos\alpha \sin\theta'$ and an additional component of x phase (dispersion mode) is generated equal to $M_0 \sin 2\alpha \sin^2(\theta'/2)$.

These trigonometric factors are exact on resonance, but for *in vivo* spectroscopy r.f. pulses will often be so weak that the factors no longer hold true off resonance across a normal spectral width. Weak r.f. pulses act along axes which are tilted by an angle α towards the main field (z) axis where α is related to the resonance offset ΔH (Hz) and 90° pulse time on-resonance t_{90}(s) by

$$\tan\alpha = 4\,\Delta H\, t_{90}. \qquad (5)$$

For any on-resonance pulse θ, the rotation angle off resonance is increased to θ' given by

$$\theta' = \theta \sec\alpha. \qquad (6)$$

Thus the vector diagram of Figure 1a translates to that of Figure 1b off resonance. The cos2θ factor for a 2θ [±x] pulse converts to $(1-2\cos^2\alpha \sin^2\theta')$ off resonance. The sinθ factor for the θ excitation pulse becomes $\cos\alpha \sin\theta'$, but in addition to this normal absorption-mode signal, an unwanted dispersion-mode signal proportional to sin2θ $\sin^2(\theta'/2)$ arises (see Figure 1b). Lastly, the off-resonance factor for a 2θ[±x,±y] pulse is $\pm\cos^2\alpha \sin^2\theta'$, where the minus sign signifies that dispersion signal is inverted by the pulse. Again, these various factors must be multiplied together for each pulse in a sequence, and although the result may be complicated, calculations as a function of θ and ΔH need to be carried out for each prospective method to check its extent of validity off resonance. For example, it is found that apart from eventual loss of signal intensity off resonance, accurate T_1 values can be measured

using sequence (3), and any spin-echo method can be employed with sequence (4).

A fourth and final building block for our pulse sequences, $2\theta[\pm x,\overline{0}]$, is derived by subtracting the result of two transients, obtained using just θ; acquire, from sequence (3) giving

$$2\theta[\pm x,\overline{0}] - \tau - \theta; \text{ acquire} \qquad (7)$$

where $\overline{0}$ signifies that the pulse is not applied and the receiver phase is inverted. The trigonometric factor for a $2\theta[\pm x,\overline{0}]$ pulse applied before the θ excitation pulse is $\sin^2\theta$ on resonance and $\cos^2\alpha \sin^2\theta'$ off resonance, and so it has the same quantitative effect as a $2\theta[\pm x,\pm y]$ pulse used after θ except that dispersion signals are not inverted. This equivalence between $2\theta[\pm x,\overline{0}]$ and $2\theta[\pm x,\pm y]$ holds true no matter whether 2θ is a hard, shaped or composite pulse (13).

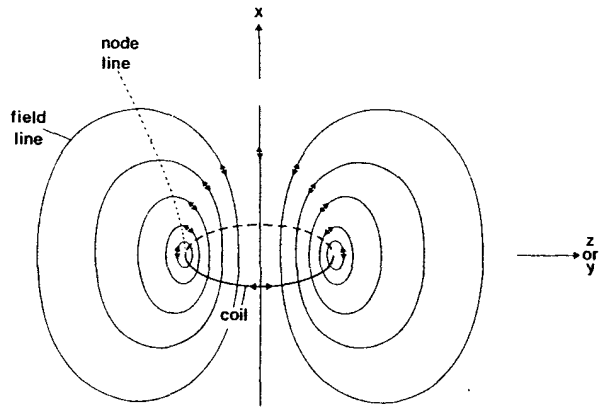

Figure 2. The r.f. field lines produced by a surface coil. If the plane displayed is the xz plane, there will be node lines where the r.f. field lines are parallel to z, the external magnetic field direction.

III. THE R.F. FIELD OF THE SURFACE COIL

The basic surface coil is one or more circular turns of wire connected to a tune and match network. During an r.f. pulse a large oscillating current flows in the wire and this induces an oscillating magnetic field (or r.f. field) along the same field lines as the magnetic field produced by a direct current in the coil. Clearly the r.f. field is strongest closest to the coil wire as depicted in Figure 2.

As described in the early report by Ackerman et al (14), the r.f. field produced by any coil consisting of continuous wire may be calculated by using the Biot Savart Law to determine the magnetic field produced by direct current in the coil. Detailed three-dimensional calculations have been published (4,7,15,16) and these are illustrated in Figure 3a and d. The calculated field in Figure 3a is given in terms of pulse angle contours assuming $\theta = 90°$ at 1.0 radius depth. One half of the xy plane through the center of the coil is shown with the vertical axis being the coil axis or x axis. After a single θ pulse the signal response from each volume element is given by $\theta\sin\theta$, where the θ term accounts for the decreasing sensitivity of the coil to volume elements further away from it. Thus signal will be detected from all points in sample space except where $\theta = 180, 360° \ldots$, and the signal will be positive for $\theta \sim 90°$, negative for $\theta \sim 270°$ and so on as indicated.

The shape of the r.f. field may also be revealed by experiment. The images in Figure 3b and c were obtained by adding pulsed field gradients to sequence (4) and imaging the signal response from a slice phantom of H_2O [eg. see Ref. (17)]. The signal response is consequently given by $\theta\sin^3\theta$, yielding similar banded results to that shown in Figure 3a but with more diffuse boundaries. For Figure 3b, θ was set at 90° at about 1.0 radius depth to mimic Figure 3a, but in Figure 3c the pulse lengths have been more than halved to illustrate that these banded areas can be pushed to variable depth into the sample. Note the lower sensitivity to the 90° signal region in Figure 3b compared to the 270° region ($\sim$ 3 times as intense) and the 450° region ($\sim$ 5 times as intense) as determined by the θ sensitivity term. However, because the volumes of these "high flux" regions become smaller with increasing pulse angle, their total contribution is of a similar magnitude to the 90° region, and for simplicity we generally ignore the θ sensitivity term in

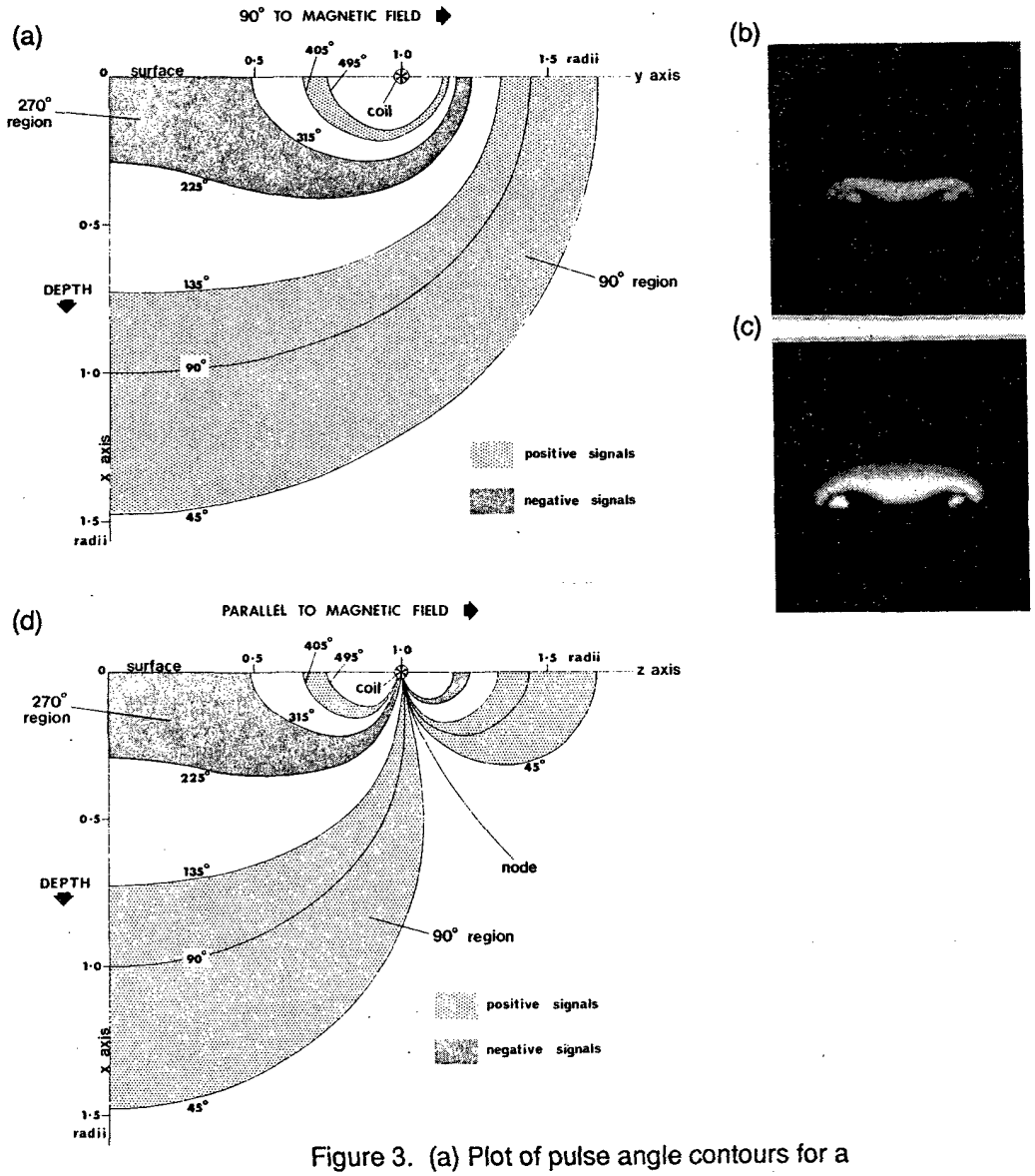

Figure 3. (a) Plot of pulse angle contours for a surface coil for the xy plane (transverse to the external magnetic field). The shaded areas correspond to regions from which signal would be detected using an appropriate depth pulse sequence (e.g. signal given by $\cos^2 2\theta \sin^3\theta$ for the depth pulse $(2\theta[\pm x])_2;\theta;\ 2\theta[\pm x,\pm y]$;acquire as described in section VI). A 90° pulse is assumed at 1.0 radius depth, but any other pulse angle can be accounted for by scaling the values given. The pulse angle contours also correspond to sensitivity contours. (b) Experimental image of the sensitive volume in the xy plane of a surface coil obtained by Ordidge (18). (c) As for (b) with all pulse lengths divided by 2.5. (d) As for (a) for the xz plane (parallel to the external magnetic field).

theoretical expressions such as $\theta\sin^3\theta$.

In an NMR experiment, the active component of the r.f. field is the oscillating component at right angles to the external field axis (z). For the xy plane displayed in Figs 3a to c the r.f. field is always transverse to the z axis. However, from Figure 2 it can be seen that in the xz plane there is a node line where the r.f. field is parallel to z and no NMR signal can be excited or detected. The calculated result for the xz plane is shown in Figure 3d, which demonstrates that this node line further complicates the shape of the sensitive volume.

The normal situation for a surface coil as illustrated in Figure 3 is clearly unsatisfactory. When trying to sample regions at a modest depth into the sample, intense high flux signals are generated near the surface, and even if these can be suppressed, the 90° region curves back into the surface outside the circumference of the coil.

Obviously, additional means of sensitive volume localization are required whenever it is necessary to study a region beneath a surface layer.

IV. MAXIMIZATION OF SIGNAL-TO-NOISE

Haase et al (15) and Evelhoch et al (16) have extended the theoretical calculation of distribution of surface coil signal intensity to include the relaxation time T_1, and the time for each transient, TR. At high repetition rates, say $TR = 0.05T_1$, and reduced pulse lengths, the distribution of signal intensity is significantly altered with less high flux signals near the surface and more signal intensity at one radius depth, ie. a more uniform distribution of signal, and total signal intensity is doubled for optimum pulse lengths at these high repetition rates. However, despite the improvements at higher repetition rate, the signals from an intervening surface layer would still swamp an inner organ by a factor of 3 to 9 times, ie. additional methods are definitely required in such cases.

In maximizing total signal-to-noise, the approach of Evelhoch et al (16) is valid for experiments where a thick surface layer is to be detected, or where an underlying layer is detected but the intervening surface layer does not contribute any interfering signals. Improvements can also be obtained in signal-to-noise ratio without increasing the repetition rate of the experiment (and disturbing the normal ratio of spectral peak lines), by using a composite excitation pulse θ which provides for uniform excitation of transverse magnetization across a range of pulse angles around $\theta = 90°$. However, contrary to some published claims (3), the simplest composite 90° pulse introduced by Freeman et al (19), $\theta = \theta[x];\theta[y]$, does not increase signal-to-noise, since the additional signal components which are generated are entirely dispersion-mode, have different phases either side of $\theta = 90°$, and so mutually cancel. Nevertheless, Tycko et al (20) have described pulses which provide uniform excitation across a factor of three variation in pulse angle and which have a much reduced phase problem. These should prove useful.

Hetherington et al (21) have used the $\theta[y];\theta[x];\theta[-y];\theta[x]$ composite pulse of Levitt and Ernst (22) and have achieved a 20% increase in signal-to-noise in surface coil studies of the rat brain. Although this composite 90° pulse does produce dispersive components, Hetherington et al eliminated these by using the phase-cycled equivalent $\theta[-y];\theta[x];\theta[y];\theta[x]$ for alternate transients.

Hetherington et al have also extended the use of composite pulses to spin-echo sequences and surface coils, with both the θ excitation pulse and the 2θ refocusing pulse replaced by composite pulses, and achieved a 40% increase in signal-to-noise over simple pulses. This however requires a more complex but nevertheless general phase cycling scheme of the 2θ refocusing pulse, than that shown in sequence (4), as determined by Hetherington and Rothman (23).

Recently we have developed a complex excitation pulse where amplitude and frequency are continuously modulated during the pulse as sine and cosine functions (eg. from $\sin 0°$ to $\sin 90°$). This "sin/cos" pulse operates under conditions known as "adiabatic half passage" in traditional NMR and our results (24) show that it can be used under practical conditions with surface coils and that it will excite more than 90% of z magnetization to give absorption-mode signal across a variation of at least a factor of 10 in the

strength of the r.f. field. Further preliminary calculations (25) indicate that if the length of the "sin/cos" pulse is doubled (e.g. to extend from sin 0° to sin 180°), a 180° inversion pulse of similar efficiency is produced. This sin/cos pulse appears to be somewhat shorter but gives similar results to the "sech/tanh" pulse previously described by Silver et al(26). But both these adiabatic pulses introduce very bad phase problems if utilized in spin-echo sequences. However our most recent calculations indicate that suitable 180° refocusing pulses can be formed by reversing the amplitude and frequency modulation to give cos/sin and tanh/sech pulses, with the former again having a length advantage over the latter. These pulses have not been exploited in *in vivo* applications, but there appears to be good prospects of being able to maximize signal-to-noise even with inversion-recovery and spin-echo sequences.

V. LOCALIZATION USING PULSED FIELD GRADIENTS

A. Selective Pulses in Pulsed Field Gradients

From Figure 3 it is clear that when using a surface coil to detect a region below the surface it is necessary to discriminate against the surface layer. This may be achieved by applying a selective pulse in a pulsed field gradient, where the gradient axis is the surface coil or x axis, so generating a selected slice which is parallel to the plane of the coil. The center of the slice should closely coincide with $\theta = 90°$ on the coil's axis, in which case the r.f. inhomogeneity of the coil will limit the lateral dimensions of the selected slice to about the diameter of the surface coil. The sensitive volume would be disc-shaped, centered on the coil's axis and flattened along the z dimension (because of the r.f. node line). This general method has been proved using a phase-cycled pulse (a depth pulse (7,27,28)], but usually the shaped pulses commonly employed in NMR imaging will be more convenient. There are numerous types of shaped pulses that may be used, and this is a rapidly developing area of research. The interested reader is referred to recent articles (29-33) and numerous preliminary reports in the abstracts of recent international conferences.

A major problem with pulsed field gradients is that eddy currents are generated in the surrounding metal of the probe and magnet which die away exponentially, thus slowing down the gradient switching. These eddy currents can be compensated electronically but a short delay of about 10 ms is normally required before signal acquisition, otherwise the resolution of the final spectrum will be reduced. During this delay, the magnetization in the selected slice must be preserved by some means, and this is discussed below in more detail. A second limitation of selective pulse/field gradient methods is that the spatial frequency shifts are mixed with the natural chemical shifts, thus generating a spread of localized slices depending on the magnitude of the chemical shift. This problem is reduced by using maximum field gradient strength, but this increases eddy currents. The effect is most significant for larger bore, higher field strength magnets and is a serious problem for ^{13}C NMR, whilst being partially limiting for ^{31}P NMR and to lesser extent for ^{1}H NMR. Both these problems will increase with the progressive move to higher field whole-body magnets.

There are three possible ways of using selective pulses:

1. Selective excitation pulses . Denoting a selective pulse in a field gradient along the x axis as θ_{SX}, a straightforward experiment would appear to be

$$\theta_{SX}[x];SL[y];\ \text{acquire}, \qquad [8]$$

where the θ_{SX} pulse has x phase. SL[y] is a spin-lock pulse of y phase, and is included to lock and so preserve the selected magnetization during the eddy current decay period. Although the use of a spin-lock pulse in this way has been proved by experiment (7,27,28), to retain its simplicity this method requires a shaped excitation pulse which does not permit the nuclear spins to dephase in the transverse plane during the pulse as a result of their natural chemical shift and the imposed spatial frequency shift. Unfortunately, such shaped pulses which do not show the dephasing

problem have yet to be devised.

Bottomley et al (34, 35) have obtained good results from the human brain by applying a sinc 90° pulse in a field gradient then acquiring the NMR signal immediately after (or slightly before) the nuclear spins are rephased by a reverse gradient. Thus no τ delay period was used to allow eddy currents to decay, but the eddy current problem was avoided by minimizing the usual coupling between the gradient coils and the surrounding metal magnet by using 0.6 meter diameter field gradient coils in their 1.5T/1 meter bore magnet. This is a proper solution but is not generally applicable to smaller bore magnets as used for animal systems, or higher field systems. Note that the effects of natural chemical shift occurring during the sinc 90° pulse and the reversed gradient are not refocused and the final spectrum will have a large phase roll which when corrected can lead to considerable spectral distortions. Bottomley et al used a cylindrical NMR transmit coil and a surface receive coil, and this aspect of their work is discussed further in section VIII, B, 2. However, as can be appreciated from Figure 3, the extent of the slices parallel to the surface coil depends only on the sensitivity of the surface coil as a receiver, and this sensitivity decreases gradually in the y direction, giving poor localization in this direction.

2. Selective inversion pulses. Ordidge and co-workers (36) have proposed the use of selective inversion pulses, $2\theta_S$, in place of 2θ in sequence (7) to select a slice parallel to a surface coil and have obtained ^{31}P brain spectra in this way. The τ delay of sequence (7) becomes the eddy current decay period, and this method has the advantage that the selected magnetization is lost via T_1 relaxation during τ, the slowest possible relaxation mechanism. Additional $2\theta_S$ $[\pm x,\overline{0})$ pulses can be added with field gradients in the y and z direction to select slices in each of the three spatial dimensions and thus a cuboid sensitive volume:

$$2\theta_{SX}[\pm x,\overline{0}];2\theta_{SY}[\pm x,\overline{0}];$$

$$2\theta_{SZ}[\pm x,\overline{0}] - \tau - \theta; \text{ acquire.} \qquad (9)$$

The $\pm x$ phase alternations remove unwanted transverse signals, although these are partially eliminated by dephasing in the pulsed field gradients. For ideal 180° and 90° pulses, as supplied by a homogeneous r.f. coil, these transverse signals will be small and so the dephasing is sufficient to allow the $\pm x$ alternations to be omitted. Thus the 64-transient cycle of sequence (9) becomes an 8-transient cycle:

$$180°_{SX}[x,\overline{0}];180°_{SY}[x,\overline{0}];$$

$$180°_{SZ}[x,\overline{0}] - \tau - 90°; \text{ acquire.} \qquad (10)$$

This is the method recently used by Ordidge et al (37) for localized *in vivo* ^{1}H NMR using a cyclindrical r.f. coil.

A disadvantage of these methods is that spins outside the selected volumes are excited by the θ or 90° pulse, and the resulting large signals are only eliminated by the alternate addition and subtraction of the detected signal. Instrumental instabilities and movement of the live sample means that such subtractions can never be perfect and random errors, or "subtraction noise" results. For the applications with a homogeneous r.f. coil, these large signals outside the selected region can be removed by using 90°; $90°_S[\pm x]$ or $90°_S[\pm x]$; 90° in place of each $180°_S[x,\overline{0}]$ in sequence (10) for example. The hard 90° pulse would generate transverse magnetization outside the selected slice which would be substantially dephased and so eliminated by the pulsed field gradient applied during the pulse. However this combination of hard and shaped pulses as proposed by Young (38) is presently prevented by the dephasing of spins during the shaped pulse (noted above for selective excitation pulses).

Aue and coworkers (39,40) have developed a partial solution to this dephasing problem by using a sandwich of soft and hard pulses, $45°_S[x]$; 90°[-x];$45°_S[x]$ (first introduced by Post et al (41) for imaging), which is equivalent to $90°_S[x]$; 90°[-x]. This sandwich corresponds to the zero part of $180°_S[x,\overline{0}]$ and the 180° inversion part is obtained using the second sandwich, $45°_S[-x]$;

$90°[-x]; 45°_S[-x]$. However, although the dephasing of spins during the $45°_S$ pulses is refocused and eliminated in the first sandwich, the problem remains for the second sandwich. Calculations also show that significant signal is generated outside the selected slice when the 90° pulse in these sandwiches is not very hard (say >50 μsec) (42). Note also that Aue and coworkers (40) mistakenly used the sandwich, $45°_S[x];90°[x];45°_S[x]$, as the second variation and that this cannot function to properly cancel signals outside the selected slice. Furthermore, they used only a two transient cycle for the three dimensional localization experiment. This must be at least an 8 transient cycle as in sequence (10), and should probably be extended to a 64 transient cycle as in sequence (9) when using surface coils. Finally, when using surface coils the sandwiches are of the form $\theta_S/2;\theta;\theta_S/2$ and the hard θ pulse on average converts only half of the detectable z magnetization outside the selected slice to transverse magnetization. Thus subtraction noise is also only reduced by half compared to using a complete $2\theta_S$ pulse.

3. Selective refocusing pulses. Having noted the equivalence between $2\theta[\pm x,\overline{0}]$ and $2\theta(\pm x,\pm y]$, a slice parallel to a surface coil can be generated using $2\theta_{SX}$ in sequence (4), and the equivalent method to sequence (9) is

$$\theta - \tau - 2\theta_{SX}[\pm x,\pm y];2\theta_{SY}[\pm x,\pm y];$$

$$2\theta_{SZ}[\pm x,\pm y] - \tau - \text{acquire} \qquad (11)$$

Although the selected spins relax via the more rapid Hahn T_2 time and the total τ delay periods are twice as long as the equivalent delay in the selective inversion methods, these spin-echo methods are applicable to small mobile ^1H metabolites for example, especially as the spin-echo helps to eliminate large fat and water signals having a shorter T_2. A second disadvantage compared to the inversion methods is that the $2\theta_S$ pulses must be accurately timed to be at the effective center of the pulsed field gradients to achieve refocusing of the selected spins. An advantage is that the large signals excited outside the selected volume by the initial θ pulse are dephased and reduced by the pulsed field gradients, so subtraction noise is less serious. Again, the $[\pm x,\pm y]$ alternations are included for surface coil studies to remove transverse error signals, but since these are small enough for homogeneous r.f. coils to be efficiently dephased by the pulsed field gradients, sequence (11) reduces to

$$90° - \tau - 180°_{SX}[x,y];180°_{SY};$$

$$180°_{SZ} - \tau - \text{acquire, receiver}[+,-]. \qquad (12)$$

One phase alternation is retained to eliminate any residual signal excited by the 90° pulse and not dephased by the field gradients, giving a final 2-transient cycle. Though previously suggested (43) these methods have yet to be exploited, although Ordidge (36) has combined similar sequences with selective excitation pulses, a technique that has now been superceded.

B. Two-Dimensional Fourier Transform Localization

1. 2DFT localization. As introduced by Maudsley and coworkers (44) and further described by Haselgrove et al (45), an incremented pulsed field gradient can be employed in the first τ period of a spin-echo (sequence (4) for surface coils), and a second Fourier transform provides separate spectra from a series of slices perpendicular to the gradient axis (x axis for surface coils). In general, the method has significant advantages over slice-selective pulses because spatial frequency shifts and chemical shifts are not mixed, and because weaker gradients can be used leading to less problematical eddy currents. For a surface coil, the transaxial extent of the slices is limited by the usual $\theta\sin^3\theta$ dependence of signal intensity for sequence (4). Thus only a field gradient in one dimension (along the coil's axis) is required, so avoiding the usual long acquisition time requirements of multi-dimensional chemical shift imaging. The use of one incremented gradient in this way is the same as the use of an incremented phase-encoding gradient in normal

imaging, so this procedure is well established.

2. Selective 2DFT localization. Referring back to Figure 3, it would seem that only a few incrementations of a gradient along the coil's axis would be necessary to generate a convenient thick slice at some depth (centered on $\theta = 90°$) and discard the slices closer to the surface. Unfortunately, normal slices (or pixels) have a sinx/x signal dependence relative to the x gradient dimension and adjacent slices are not well resolved (46). More gradient incrementations could be used to generate thinner slices and one well resolved thick slice could be obtained by summing N thinner slices. But this leads to a signal-to-noise penalty of $N^{1/2}$ (47,48). Mareci and coworkers (49-52) have solved this problem by showing that if a variable number of transients, weighted according to a Gaussian function, are obtained at each setting, the final slices obtained after the second Fourier transform will be Gaussian shaped. Maximum signal-to-noise is maintained at the center of such slices and only a few gradient incrementations are required to generate a thick slice, at some depth relative to a surface coil, uncontaminated by surface signals. There appears to be no clear disadvantages for this selective 2DFT method and it is likely to be widely used in its own right or in conjunction with depth pulses (section VI) or even uniform excitation methods (section IV) to generate a series of slices with maximum signal-to-noise.

C. Sensitive Point Steady-State Free Precession Method

This technique, which utilizes r.f. pulses with a rapid repetition rate applied in the presence of slowly alternating field gradients (53-58), requires further development before its value can be assessed. However it would seem that complete localization could be obtained using the sensitive point method with a surface coil by generating a selected slice perpendicular to the single alternating field gradient along the coil's axis.

VI. LOCALIZATION USING RADIOFREQUENCY INHOMOGENEITY

A: Rotating Frame Zeugmatography

By incrementing a single excitation pulse length during a series of transients, and applying a two-dimensional Fourier transform, a series of spectra can be obtained from curved slices whose boundaries are determined by pulse angle contours as in Figure 3. Hoult (59) described the basis of this method which was further developed by Cox and Styles (60) and recently discovered by Bolton (61). Haase et al (62) introduced the technique to surface coils and Garwood et al (63) used it to obtain ^{31}P metabolite maps from a bovine eye. This imaging method is analogous to normal 2DFT imaging (section V, B) with the difference that the incremented magnetic field gradient is replaced with an incremented r.f. field gradient. Extending this analogy, each slice (or pixel) will show poor resolution and their summation leads to much less signal-to-noise than can be obtained by other methods (eg. depth pulses - next section). However, a weighted summation can be used to optimize signal-to-noise, as in the selective 2DFT method, and this leads to the Fourier series window technique described below (section VI, D).

B. Simple Depth Pulse Sequences

1. Design. Depth pulse sequences may be used to obtain spectra with maximum signal-to-noise from single curved slices whose boundaries are determined by pulse angle contours as in Figure 3 (4-7,11, 27, 28, 64-67). These sequences have been reviewed (5) and improved (6) and are formed from the phase-cyled pulses of sequences (3) and (4), giving in general

$$(m\times 2\theta[\pm x])_n; \{\Sigma \ell \times \theta\}; 2\theta[\pm x,\pm y]; \text{acquire} \qquad (13)$$

A $2\theta[\pm x]$ type pulse may be used as a fraction or multiple, $m\times 2\theta$ (eg. $\theta/3[\pm x]$ or $4\theta[\pm]$), and so, for example, the on resonance factor is $\cos(m\times 2\theta)$. Often, several of these pulses are useful (with different values of m) as signified by the subscript n. The excitation pulse θ may also be

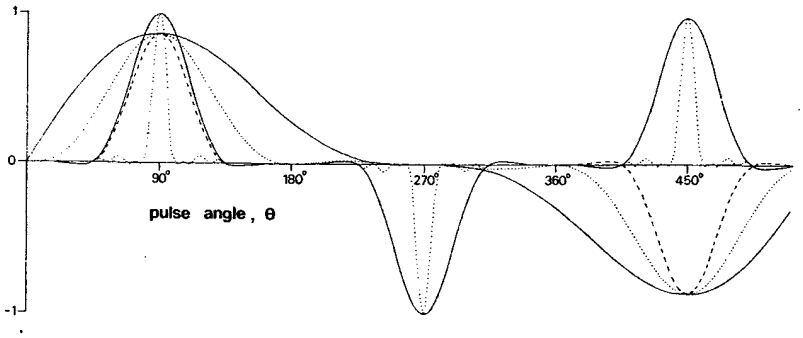

Figure 4. Signal magnitude versus pulse angle for various depth pulses. Some examples show the 270° signal region suppressed, but in all cases both 270° and 450° signals can be readily eliminated, by modification of the depth pulse, with a small reduction (up to 20%) in signal intensity at θ=90°. The continuous curve with 270° and 450° signals retained corresponds to the shaded signal regions in Figure 3.

used as a fraction or multiple, as indicated by $\ell \times \theta$, and several values of ℓ may be used with the results of the various transients summed as a linear combination using calculated coefficients (hence Σ). Lastly, if significant unwanted dispersion signals occur for any sequence, these can be entirely removed by repeating sequence (13) with $2\theta[\pm x,\overline{0}]$ at the beginning, in place of $2\theta[\pm x,\pm y]$ at the end, and summing the results. A selection of the range of possibilities is illustrated in Figure 4. A single θ pulse would be represented by a sinθ curve, so compared to this, the limits of signal intensity around $\theta = 90°$ can be pushed in to a variable degree, and this can be achieved with or without the complete removal of 270° and 450° high flux signals. In terms of Figure 3, the high flux signal regions can be eliminated and the 90° signal region can be narrowed or expanded at will. T_1 measurements can be made by inserting an inversion-recovery τ delay after an initial $2\theta[\pm x]$ pulse, and any spin-echo method can be applied by inserting τ delays on either side of the $2\theta[\pm x,\pm y]$ pulse in sequence (13).

2. Off-resonance effects. For *in vivo* work we have noted that a consideration of off-resonance effects is very important. These have been calculated for all depth pulses using the trigonometric factors listed in section II, and a typical result is shown in Figure 5a. This has been calculated by substituting $t_\theta \times 90/\theta$ for t_{90} in equation (5) to allow for the variation of t_{90} throughout sample space. We have found such plots to be more informative than previous versions where the resonance offset axis, ΔH, was given in terms of reciprocal t_{90} (68), In Figure 5, the frequency offsets can be obtained by substituting for the length of the θ pulse, $t_\theta(s)$, used. In all cases it is found that r.f. discrimination is retained off resonance, but there is a gradual loss of signal intensity , with the depth pulses useable to where signal drops to say 50% of maximum, at about $0.1t_\theta^{-1}$

Recently, Shaka and Freeman have also noted the utility of $m\times 2\theta[\pm x]$ pulses which they called prepulses (69,70). Shaka and Freeman (70) did however introduce a new type of phase cycled

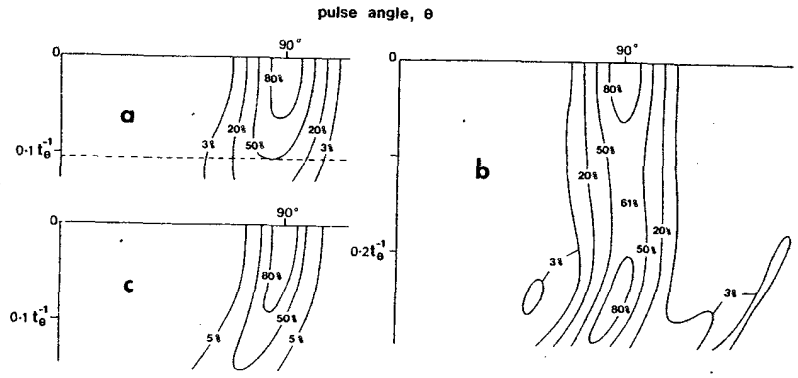

Figure 5. Contour plots of signal intensity (total transverse magnetization) against pulse angle θ and frequency offset for (a) depth pulse [I] of refs. (5, 6) (the off-resonance characteristics are typical of simple depth pulses), (b) a sequence equivalent to depth pulse [I] on resonance but having all simple phase-cycled pulses replaced by composite phase-cycled pulses as according to Shaka and Freeman (70) and (c) a 9 term FSW with dispersion signals removed. In some cases the off-resonance properties of simple depth pulses can be modestly improved to give similar behavior to that shown for the FSW in (c).

prepulse which can be written as $4\Theta[\pm x(2/3), 0(1/3)]$, where 2/3 and 1/3 indicates that the pulse is not applied for one third of all transients. This type of pulse can be generalized to include established pulses such as $2\Theta[\pm x,\overline{0}]$ and new pulses such as $4\Theta[\pm x,0]$ and $6\Theta[\pm x(2/3),\overline{0}(1/3)]$ (68). In this way many new depth pulses can be devised but these are generally similar to established sequences or give identical results on resonance (68). However, $2\Theta[\pm x]$ pulses can be eliminated from some depth pulses using the new pulses and this may lead to a modest improvement off resonance. In such favorable cases, signal intensity extends a little further off resonance similar to Figure 5c, but the useful limits are still restricted to about $\pm 0.1 t_\Theta^{-1}$ because of the pronounced curvature of the pulse angle window to lower θ values (68).

3. Short recycle times. The localization provided by depth pulses (or any other method described in this section VI) may fail at short recycle times, TR, though we have experienced no experimental difficulty at $TR \gtrsim 2T_1$. Garwood et al (63) eliminated this problem for rotating frame zeugmatograghy using presaturation. Decorps et al (71) have shown presaturation to be generally applicable and that maximum signal is obtained at $TR = T_1$ although there is little gain over TR = (2 to 3)×T_1. However, presaturation would allow for a large range of T_1 values as occurs for *in vivo*

^{31}P species for example.*

4. Applications. All the localization methods in this section VI will provide sensitive volumes in the form of pulse angle slices. From Figure 3 it is clear that these slices will always intersect the sample surface and may not be conveniently shaped. Combined methods of localization that eliminate surface signals are described in sections VII and VIII. Nevertheless, there are important applications for depth pulses alone, especially when a modest reduction in surface signals is sufficient and when it is important to prevent detection of regions beyond a certain depth. *In vivo* applications along these lines have been described (11,66,72,73). Even with complete elimination of surface signals, the curved nature of depth pulse sensitive volumes may not seem very satisfying from a geometrical point of view compared to the more easily visualized cuboid shapes that can be generated using pulsed field gradients. But live animals do not fit well to cuboid shapes and there will be many instances where curved slices fit better, eg. surface infarcts and trauma to the brain.

Note that signal-to-noise will be a common limiting factor, especially in these early stages of the development of *in vivo* spectroscopy. For example, a simple depth pulse may easily limit signal detection to one-third of the original volume and this would require nine times more transients to acquire a reasonable spectrum. Such a penalty can often not be afforded and it has been found that depth pulses which localize to a small degree (eg. elimination of high flux signals with minimal reduction of the 90° signal region) are important (72, 74). Along these lines, Gadian et al (75) and Decorps et al (76) have utilized the minimal extra localization provided by a $2\theta[\pm x,\pm y]$ pulse in spin-echo sequences.

C. Composite Depth Pulses

1. Narrowband inversion pulses. Shaka and coworkers (77,78) and Tycko and Pines (79) have described some depth pulses in which one or more of the phase-cycled pulses are composite narrowband inversion pulses. The basic method is described by sequence (4) or (7) (with $\tau = 0$) where 2θ is now the composite pulse. Our experiments and calculations (13,68) have shown that these composite depth pulses give similar results on resonance to some established simple depth pulses, but r.f. discrimination is lost at resonance offsets which are much less than the useful range for simple depth pulses. These composite sequences require a reduced phase cycle compared to the equivalent simple depth pulse, but this small advantage is out-weighed by the poor off-resonance characteristics of the present narrowband inversion composite pulses and consequently they are not not competitive (13).

2. Broadbanded composites. Recently, Shaka and Freeman have extended the useful range of offset frequencies of a depth pulse by substituting a new type of composite pulse for each simple pulse (except the excitation pulse) in the simple depth pulse sequence. In favourable cases (68) the offset range can be increased to $0.25t_\theta^{-1}$ and an example is shown in Figure 5b. However, these composite pulses greatly increase the length of the depth pulse and it is easily shown that simple depth pulses retain the advantage in terms of length and/or deposition of r.f. power in live tissues provided there is sufficient r.f. power to cover the required spectrum (68). This will often be the case given the large r.f. amplifiers now being employed on *in vivo* imagers/spectrometers.

D. Fourier Series Windows

1. Design. Garwood and colleagues (80) have introduced a method whereby a single pulse is incremented during a series of transients (like rotating frame zeugmatography) but the transients are summed using pre-calculated coefficients which are determined by the Fourier components of a square window. Our most recent calculations (81) show that the range of possibilities indicated in Figure 4 for depth pulses can be mimicked with these Fourier series windows (FSW's) and some of these features have also been described by Metz and Briggs (82). The ideal square shape of the window is lost because of truncation of the

*Recent results using one complete depth pulse localization method (Bendall, Foxall, Nicols, and Schmidt, *J. Magn. Reson.*, in press, 1986) showed no loss of localization at short recycle times.

Fourier series, but the "wobbles" of signal intensity on either side of the selected pulse-angle slice (caused by truncation) can be minimized to <4% as for depth pulses. Alternatively, similar windows can be generated using Gaussian coefficients (as described for the 2DFT method). The FSW's show a small loss in signal-to-noise over the equivalent depth pulse (10-15%), but they may be experimentally more convenient. In particular, there is the ability after data collection to "zoom" in from a broad window to a narrower window by discarding spectra using the longest r.f. pulses to generate the broader windows. This aspect will be useful for determining when the degree of localization is sufficient to eliminate signals from surrounding tissues.

2. Off-resonance effects. Resonance offset calculations for FSW's show that r.f. discrimination is lost beyond about $0.05\ t_{\theta}^{-1}$ because of dispersion error signals. These can be removed using

$$\{\Sigma\ell\times\theta\};2\theta[\pm x,\pm y];$$

$$\text{acquire} + 2\theta[\pm x,\overline{0}];\{\Sigma\ell\times\theta\};\text{acquire} \qquad (14)$$

as for depth pulses, where $\{\Sigma\ell\times\theta\}$ signifies the FSW and an FSN, with dispersion signals removed, is illustrated in Figure 5c indicating that the usefulness of FSN's is limited to about $0.1t_{90}^{-1}$. by the curvature to lower pulse angles. An alternative to sequence (14) is to use a spin-lock pulse to dephase the unwanted dispersion signals,

$$\{\Sigma\ell\times\theta\}[x];SL[y];\ \text{acquire}, \qquad (15)$$

a procedure previously described for depth pulses (7).

3. Related methods. An early extension of rotating frame zeugmatography to FSW's was described by Pekar et al (83), but unfortunately they chose to mimic the most inefficient depth pulse sequences. The new "very fast" methods of Pekar and coworkers (84,85) also appear to be impractical because they require a prior knowledge of T_1 times, which must be uniform across the sample and the same for each chemical species.

As in sequence (14), FSW's can take the place of some of the phase-cycled pulses in the depth pulse methods described in the following sections. It is merely necessary to replace the excitation pulse by $\{\Sigma\ell\times\theta\}$ and then omit whichever phase-cycled pulses are no longer necessary.

VII. LOCALIZATION BY COMBINING THE METHODS OF PULSED FIELD GRADIENTS AND RADIOFREQUENCY INHOMOGENEITY

1. Selective depth pulses in pulsed field gradients. The localization that can be achieved using a depth pulse may be good enough for a particular metabolic time-course study, but unless this can be proved, the data obtained is meaningless. It would be valuable to filter out the intervening surface signals using a pulsed field gradient method and if this showed that the proposed experiment was prejudiced by these surface signals then a time-course study could proceed at maximum efficiency without the field gradient. All simple depth pulses show good frequency selectivity, being similar in this regard to a Gaussian shaped pulse, and so the whole depth pulse, DP(θ), can be treated as a selective excitation pulse and applied in a pulsed field gradient. That is, DP(θ) takes the place θ_{SX} in equation (8). This combined localization method has been proven by phantom studies (7,27,28).

2. Selective 2DFT with depth pulses. The selective 2DFT method of Mareci and coworkers (49-52, section V, B, 2) can easily be combined with any depth pulse which contains a $2\theta[\pm x,\pm y]$ pulse, and these authors have demonstrated some of the possible variations (51,52). Writing a depth pulse as DP(θ); $2\theta[\pm x,\pm y]$, a simple spin-echo is appropriate as in sequence (4) with DP(θ) in place of θ and the incremented gradient inserted in the first τ period. It will be common to filter out the surface signals using an incremented x gradient, but it is also possible to divide up the 90° signal region into voxels using incremented gradients in both the y and z dimensions (5,7). Again, the gradients can be discarded if the depth pulse is

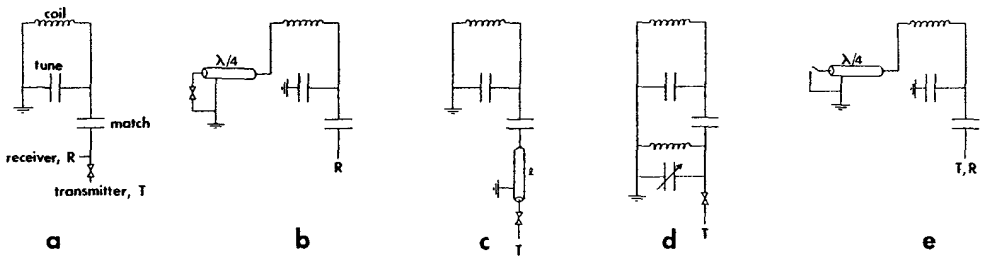

Figure 6. Circuits useful for eliminating multiple coil coupling.

proven to be sufficient.

VIII. LOCALIZATION USING MULTIPLE R.F. COILS

For a simple surface coil, the 90° region of signal intensity always curves back into the surface outside the circumference of the coil. This is true of any planar coil (including the "flux concentrator" (86, 87)). Complete localization without field gradients requires at least a second inhomogeneous r.f. coil, whose r.f. field differs markedly in shape from the first coil. The second coil may be used as a receive coil because of its different sensitivity to sample space, or the two coils may both be used as transmit coils so that the localized region is the region of overlap between the sensitive volumes of the two coils. The basis of these two methods was described in one of the original depth pulse articles (64).

A. Elimination of Multiple Coil Coupling.

1. Separate transmit/receive coils. When two r.f. coils are tuned to the same frequency, they interact and modify each other's r.f. field. For transmit/receive coils, this unwanted coupling has been removed by using crossed diodes in series with the transmit coil and in parallel with the receive coil (64). Recently we have improved on this using the circuitry in Figure 6 (88). In comparison to the normal tuned circuit depicted in Figure 6a, a $\lambda/4$ cable and crossed diodes to ground as in Figure 6b deactivates a receive coil during pulses from a transmit coil. A cable of variable length ℓ in the transmit line as in Figure 6c, or the equivalent circuit in Figure 6d, adequately detunes a larger transmit coil during signal acquisition (89). We have found that this coil circuitry is efficient even for the worst case of a surface receive coil inside and parallel to a cylindrical transmit coil. Haase (91) has also proposed a circuit of the type shown in Figure 6c, but unlike Haase we find that the length ℓ should specifically not be equal to $n\lambda/4$ (n an integar). In the case of transmit/receive coaxial coplanar surface coils it is usually unnecessary to achieve complete decoupling of the coils, because the r.f. fields are already inhomogeneous, and Styles et al have found a less efficient circuit to be adequate (90). However, the circuits of Figures 6b,c and d are general and can be used for this application too.

2. Separate transmit coils. The above transmit/receive decoupling methods are all passive - they rely on the shorting of crossed diodes during r.f. pulses. For separate transmit coils a passive method cannot be used but we have successfully employed the actively switched variant of Figure 6b as in Figure 6e (17). It was necessary to use rapid reed relays as the

switches, so this method is restricted to low frequency nuclei in small animal magnets to enable the λ/4 cables to extend outside the main magnetic field. Present research is focused on the more general circuits in Figure 6c and d with actively switched PIN diodes in place of the normal crossed diodes.* Hedges and Hoult (92) have also proposed this solution to the problem.

3. Separate coils for imaging and spectroscopy. It is extremely useful to obtain a proton image of the head or body using a circumscribing coil and then obtain a localized spectrum with a surface coil already in place. The position of the surface coil relative to the image can be calibrated using small H_2O phantoms adjacent to the coil, or better still, the sensitive volume of the surface coil (including depth pulse localization) can be displayed on the image by generating a second image using the surface coil but the same field gradient settings as for the first image (74). However, care must be taken to minimize coupling between the two coils. Normally there will be no problem if the surface coil is much smaller than the cylindrical coil and if they are orthogonal and tuned to different nuclei. If tuned to the same nucleus, one should be detuned mechanically (by missetting the tuning capacitance or inserting a switch) whilst using the other. Switches would also be necessary for non-orthogonal coils. Figure 6e would be appropriate for the surface coil or the switch should be directly in the circuit in place of the λ/4 cable. Switches substituted for the crossed diodes in Figure 6c or d should be sufficient for the larger imaging coil.

B. Separate Transmit/Receive Coils.

1. Coaxial coplanar surface coils. Experimental results obtained using a depth pulse and coaxial coplanar transmit/receive surface coils are illustrated in Figure 7 (7). High flux signals near

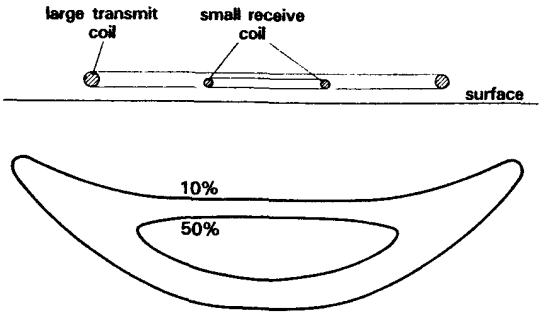

Figure 7. Signal intensity contours for coaxial coplanar surface coils. The contours have been extrapolated from the experimental results given in ref. (7). The plane displayed is the xy plane.

the surface were eliminated with the depth pulse, and the small receive coil discriminates against the 90° surface signals (outside the circumference of the transmit coil) on the basis of sensitivity, since sensitivity decreases more rapidly outside the circumference of a coil than it does along the coil's axis (see Figure 3). It is now clear that in our introductory experiment, we attempted to sample a region which was too far from the probe. The depth should be limited to less than the diameter of the small coil. This will greatly increase the sensitivity of the receive coil to the region near the coil's axis without much increase in the surface signals, thus gaining better discrimination overall and restricting signal detection to a region where the small receiver coil is reasonably efficient. Styles et al (93) have used similar dimensions to this with rotating frame zeugmatography and have obtained human liver spectra separate from the intervening muscle wall.

2. Homogeneous-transmit/surface-receive coils. When using separate transmit and receive coils there is a potential phase problem whenever the r.f. field lines of force from the two coils take different relative directions in the laboratory xy plane at different points in sample space. These different relative directions are directly transferred to the NMR experiment as phase shifts in the detected signal from the different sample points, and so signal for each chemical species

*This research showed that the circuits in Figure 6c and 6d were inadequate, but that of Figure 6e with PIN diodes in place of the reed relays has been very successful (Bendall, Foxall, Nicols and Schmidt, *J. Magn. Reson.*, in press, 1986).

cannot add coherently. This problem does not occur in the xz plane because only the r.f. field component in the x direction is active (see Figure 2). We have determined that for the coaxial coplanar surface coils of Figure 7 the phase shift is not large across the sensitive volume in the xy plane and so the problem is not serious (5, 7, 64). However the problem is severe for a large cylindrical transmit coil used with a small surface receive coil. The r.f. lines of force of the homogeneous r.f. coil can be superimposed as parallel lines on those of the surface coil in Figure 2, and so in the xy plane identical signals will cancel from two sample points where the surface coil lines of force are pointing in opposite directions (94). It has been argued that the cancellation of signal because of phase difference does itself enhance localization, but this is only true for a homogeneous sample (which is not interesting to an *in vivo* spectroscopist).

These problems represent a further limitation of the method of Bottomley et al (34,35), which can be summarized as uncertain transaxial localization depending on the homogeneity of the sample, and provide a powerful argument against using homogeneous-transmit/surface-receive coils.

C. Separate Transmit Coils

1. Coaxial coplanar surface coils. If some phase-cycled pulses in a depth pulse sequence are applied with one r.f. coil and some with another, signals will only be acquired from the overlap region of the two sensitive volumes (because the trigonometric factors discussed in section II for the various pulses are multiplied together). Such an overlap region is illustrated by the experimental image in Figure 8c, which compares to the images for the large surface coil (Figure 8a)

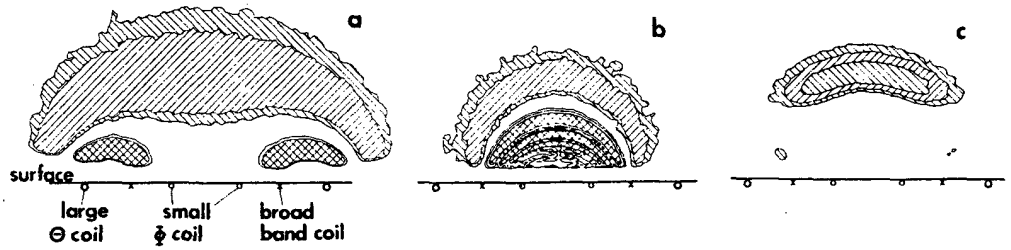

Figure 8. Images of the sensitive volumes in the xy plane obtained using a slice phantom of H_3PO_4 and the coaxial coplanar surface coils depicted (17). The small signal regions close to the coil wire in (a) are 270° regions and there is also a complicated high flux region in (b) closer to the small coil. The broad band coil is a continuous circle of wire which couples with the transmit coils and enhances the difference in shape of the two overlapped sensitive volumes.

and the small coaxial coplanar surface coil (Figure 8b) when used individually (17). An improved version of the pulse sequences used in the original study (17) is

$(2\phi[\pm x,\overline{0}])_2$ - τ - DP(θ); acquire with θ coil, (16)

where the ϕ pulses are applied with the small coil ϕ; the tuning of the coils is switched during τ; DP(θ) is a depth pulse applied with the large coil ø which eliminates the 270° signals shown in Figure 8a; and the signal is acquired with the large coil. The phase problem referred to in the previous section does not affect the application of an inversion pulse (2ϕ) by the second coil as in sequence (16), and the phase error was also avoided in the original method (17) by using double spin-echo. Note that if the degree of localization provided by the $2\phi[\pm x,\overline{0}]$ pulses is insufficient, this can be increased using narrowband inversion pulses (section (Vi, C, 1) such as the Q^1 pulse of Shaka and Freeman (77). Increased pulse power will be necessary because such pulses operate over a reduced bandwidth, and they should be applied as $Q^{\pm 1}$ or Q^{+1}; Q^{-1} to remove deleterious off-resonance effects as recently described (13, 68, 78).*

2. Homogeneous and surface transmit coils. It would seem contradictory to attempt additional localization using a homogeneous r.f. coil, but this has been proposed by Doddrell and coworkers (95). These authors went to considerable trouble to obtain "phase coherence" between a homogeneous r.f. coil (saddle) and a surface coil but as explained in section VIII, B, 2 this is not possible. Second, the effectiveness of the achieved "phase coherence" was demonstrated using a phase-alternated inversion recovery sequence like sequence (3) except that the inversion pulse was applied with the homogeneous r.f. coil and the excitation pulse with the surface coil (like in sequence (16)). However, as mentioned for sequence (16), the phase of inversion pulses relative to the excitation pulse in such alternated sequences is immaterial since no transverse magnetization is generated by them, yet, impossibly, these authors generated a substantial "out-of-phase" error in the final signal. Third, the "volume-selection capabilities" of their method was achieved primarily by matching the surface coil θ pulse to average 180° over one of two small phantom samples, the first and crudest surface-coil localization procedure ever used (96). Fourth, "excellent volume selection" was achieved by adding a "purging" 90° pulse applied with the homogeneous r.f. coil. Such a pulse can have no effect in the xz plane (as in Figure 3d), but imposes a node line in the xy plane of Figure 3a like that in Figure 3d. This improvement does not appear to be particularly worthwhile.

D. Other Coils

These multiple coil techniques are general methods and there are good prospects for improved modelling of localized regions. For example, two surface coils could be used on opposite sides of the head with the overlapped sensitive volumes at a variable distance in between, or one coil could produce a curved sensitive volume just inside the skull on the opposite side of the head close to a small moveable surface coil. There is also a vast range of possiblities for using coils which are differently shaped to the flat surface coil. Preliminary results have been described for the saddle surface coil (97) and "floppy" surface coils (98), and several groups are calculating r.f. field profiles for various shapes (97, 99). The sectorial loop-gap resonator looks promising (100). As a further example, an array of four mutually orthogonal surface coils (with a common intersection point like an open four-petaled flower) can be used to produce a discrete sensitive volume which curves away from the surface (101). R.f. fields may also be shaped by introducing passive coils which couple with the transmit coils. An example is the circle of wire (broad band coil) indicated in Figure 8, and Holcomb and Gore (98) have also made use of "satellite" coils to modify r.f. fields.

*Better control of the shape of the localized volume has been recently obtained using further improved versions of sequence (16) (Bendall, Foxall, Nicols and Schmidt, *J. Magn. Reson.*, in press, 1986).

IX. HETERONUCLEAR METHODS WITH SURFACE COILS

A sequence of r.f. pulses applied to two J-coupled heteronuclei can be used to transfer information or properties from one nucleus to its J-coupled neighbor. For *in vivo* NMR, the most important applications are to ^{1}H-^{13}C systems, especially when using ^{13}C-enriched compounds, bu there are other possibilities, e.g. ^{1}H-^{15}N systems, and ^{1}H-^{19}F systems as exist in anaesthetics. A vital aspect of the ^{1}H-^{13}C and ^{1}H-^{15}N methods is that the weak ^{13}C signal can be enhanced, or the properties of the ^{13}C nucleus can be transferred to the ^{1}H nucleus and the ^{1}H signal can be detected with much greater sensitivity. The various pulse sequences fall into one of two classes, polarization transfer and spin-echo methods and a recent finding, additional to our knowledge of these heteronuclear methods within mainstream NMR, is that both the polarization transfer and the spin-echo sequences may at the same time be used for localization using depth pulse principles (102, 103).

A. Polarization Transfer

1. Localization using r.f. inhomogeneity plus signal enhancement. Polarization transfer from ^{1}H to ^{13}C leads to a factor of four signal enhancement for the ^{13}C signal. The most conservative way in terms of pulses to achieve this is to use the DEPT sequence (104) which for surface coils is (102, 105)

$$\begin{array}{lccccccc} ^{1}H & \phi[x] - (2J)^{-1} - 2\phi[\pm x,\pm y] & - & (2J)^{-1} & - & \phi/2[y] & - & (2J)^{-1} - |\text{dec.} \\ & | & & | & & | & & (17) \\ ^{13}C & \theta & & 2\theta[x,y] & & & & |\text{acq.} \end{array}$$

The ^{1}H decoupling is optional. For simplicity, the first two ^{1}H pulses and the ^{13}C pulses can be regarded as comprising spin-echo sequences as in sequence (4), hence the phase cycling of the 2ϕ and 2θ pulses, though we have recently found that half the phase cycling for the 2θ pulse is redundant as shown (105). If applied with a double-tuned surface coil with $\phi = \theta$ for maximum signal, the spatial distribution of signal will be similar to that depicted in Figure 3a and d. If applied with two coaxial coplanar surface coils, where the larger θ coil is the ^{13}C transmit/receive coil and the ϕ coil is the ^{1}H transmit coil, complete localization can be achieved like that shown in Figure 8 by adding additional phase-cycled pulses to sequence (17) using normal depth pulse principles. For example a $2\phi[\pm x]$ pulse and $\theta/3[\pm x];(2\theta[\pm x])_2$ pulses in front of the ϕ and θ pulses respectively of sequence (17) would be sufficient. This general method has been proven experimentally (102).

2. Spectral editing. DEPT may be used to edit *in vivo* ^{13}C spectra into CH, CH_2 and CH_3 spectra (106,107), but there is a considerable signal-to-noise penalty if this is done with surface coils (108), so the spin-echo method of section B below is preferable. By reversing the ^{13}C and ^{1}H labels in sequence (17) to give inverse DEPT (109), ^{1}H spectra of only ^{13}C enriched metabolites can be obtained with a factor of up to 16 enhancement in sensitivity over normal ^{13}C NMR. This is useful for ^{1}H resonances close to H_2O, but otherwise the spin-echo method of section B gives a larger sensitivity gain.

3. Localization using pulsed field gradients. Pulsed field gradient localization methods can be readily combined with sequence (17). For example, incremented field gradients can be inserted into the first $(2J)^{-1}$ period (or if necessary an extended first delay period (110)) to enable the selective 2DFT method (section V, B, 2). Alternatively, Aue et al (111) have shown that if a selective inversion pulse in a pulsed gradient (section V, A, 2) is applied to the ^{1}H spins prior to DEPT, the small spread of ^{1}H chemical shifts does not cause

a significant spread of localized regions as would result from selective ^{13}C methods (see section V, A). Thus for example, using either method, a well-localized ^{13}C spectrum can be obtained with maximum signal-to-noise using a homogeneous cylindrical ^{1}H coil (in place for ^{1}H imaging) and a ^{13}C surface coil, with a single pulsed field gradient along the surface coil's axis. There are as usual several other permutations.

B. Heteronuclear Spin-Echo Techniques.

1. General methods. Without exception, any of the pulse sequences described in this review are already spin-echo sequences, or can be converted to spin-echo sequences suitable for inhomogeneous r.f. coils, by the addition of - τ - $2\theta[\pm x,\pm y]$ - τ - (4). For a surface coil, the gated on version of the well known gated-decoupled spin-echo experiment for a coupled AX system can be written as

2. Editing of ^{13}C spectra. If $A\equiv{}^{13}C$ and $X\equiv{}^{1}H$ in sequence (18) and alternate transients are accumulated into separate computer memory blocks, then addition of the two blocks yields a methylene/quarternary subspectrum and subtraction yields a methyl/methine subspectrum. This valuable simplification of the ^{13}C spectrum is obtained in the same time as a normal spectrum (112-114) and the benefit to *in vivo* spectroscopy has recently been established in a study of ^{13}C-enriched organs (107).

3. Editing of ^{1}H spectra. If $A\equiv{}^{1}H$ and $X\equiv{}^{13}C$, a spectrum of only those protons attached to ^{13}C nuclei can be obtained by subtraction of alternate transients. This has obvious applications in ^{13}C-enrichment studies and benefits from a large potential gain in signal-to-noise over conventional ^{13}C spectroscopy. The maximum possible gains are factors of 64,128 and 192 for CH, CH_2 and CH_3

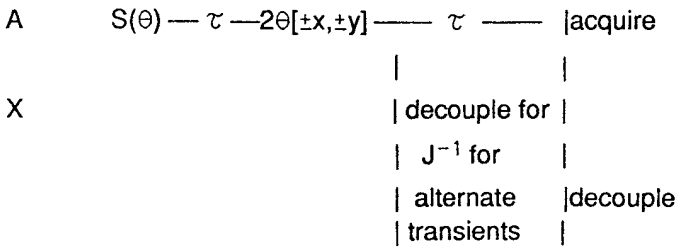

(18)

Decoupling is optional during signal acquisition. The alternative gated off version may also be used. S(θ) is the rest of the pulse sequence, and may be just θ or any depth pulse (phase-cycled, composite or FSW), or a selective pulse sequence utilizing a pulsed field gradient. The $2\theta[\pm x, \pm y]$ refocusing pulse may be any sort of composite pulse or selective pulse in a pulsed field gradient. The spin-echo may be part of an imaging sequence using incremented field gradients for the selective 2DFT method. The pulsed field gradients can be used to achieve complete localization in the various normal ways (section V). The τ period may be much longer than J^{-1} to facilitate suppression of water and fat signals by T_2 relaxation.

moieties, though experimentally there are various losses, including subtraction inaccuracies (or "noise"), which lead to much lower gains. Nevertheless, Rothman et al (115) obtained an 11-fold increase in sensitivity for the CH_3 of lactate and a 6-fold increase for the CH_2 of glutamate in the rat brain *in vivo* during a continuous infusion with ^{13}C-labelled glucose. By comparing the ^{1}H resonance of just the $^{13}CH_n$ spectrum to the ordinary spectrum ($^{12}CH_n$ + $^{13}CH_n$), the fractional enrichment was also determined. Modern stable instrumentation should give further sensitivity gains.

4. Editing of ^1H spectra plus localization using r.f. inhomogeneity. The detection of only those protons attached to ^{13}C nuclei was first introduced using a pulse on the ^{13}C nucleus rather than gated decoupling (116,117). Including a larger τ period suitable for various purposes, the pulse sequence for surface coils is

$$\begin{array}{lll} ^1H & DP(\theta) - \tau - 2\theta[\pm x,\pm y] - \tau - & |\text{acquire} \\ & | & | \\ ^{13}C & |-J^{-1}-2\Phi_C[x,\bar{0}] & |\text{decouple} \end{array} \qquad (19)$$

The $2\Phi_C[x,\bar{0}]$ pulse is a composite narrowband inversion pulse of the type describe by Shaka et al (77) or Tycko and Pines (79), or simpler versions given by us (103), and is applied for alternate transients with receiver phase alternation. $DP(\theta)$ is any depth pulse sequence, including a Fourier series. We recently proved, using phantom samples, that sequence (19) allows complete sensitive volume localization like that shown in Figure 8 when using separate $^1H(\theta)$ and $^{13}C(\phi)$ surface coils (103).

X. HOMONUCLEAR ^1H SPECTRAL SIMPLIFICATIONS WITH SURFACE COILS

A. Water Suppression

The water resonance is so massive compared to millimolar metabolites that its broad base covers the whole ^1H spectrum. Presaturation with low power single frequency r.f. is commonly used, but whilst this is efficient at the center of the H_2O signal, a significant proportion of the broad wings, which result from field inhomogeneity, remains. These wings can be removed with reasonable efficiency if the method in use includes receiver phase alternation (115) (as in sequence (19) or (20) for example), but this will lead to subtraction noise. Williams et al have used a Carr-Purcell-Meiboom-Gill (CPMG) pulse train but this is not suitable for surface coils and a simple Hahn echo does not provide sufficient H_2O suppression (118). Binomial water suppression (119-121) functions by not exciting the H_2O resonance but excites resonances within an adjustable window on either side of the H_2O resonance. Brindle et al (122) have used binomial water suppression for both pulses in a spin-echo sequence and Hetherington et al (123) have shown that this can be applied with a surface coil. Indeed it can be shown using rotation matrices (6) that every pulse in a depth pulse sequence may be split into a binomial sequence (124) so that H_2O is never excited, and recent experience shows that these binomial methods are easily efficient enough for *in vivo* ^1H NMR with surface coils (74,123).

B. ^1H Spectral Editing

1. Selective decoupling. Despite the ability to suppress the H_2O resonance, the ^1H spectrum is still mostly intractable because of large broad multicomponent fat resonances and numerous overlapping ^1H metabolites. However, Rothman et al (125) have used an editing technique of Campbell and Dobson (126) to individually detect the resonances of alanine, lactate, glutamine and glutamate in excised leg muscles and heart of a rat and to observe alanine, β-hydroxybutyrate, glutamate and glutamine in a perfused mouse liver. Williams et al (118) have since used the same method to detect the build up of lactate in a rat leg during ischemia. Although these studies were done usino homogeneous r.f. coils. Rothman et al have also used the method to reveal lactate in the *in vivo* rat brain using a surface coil, for which the editing experiment is

$$\begin{array}{lll} ^1H & \theta - (2J)^{-1} - 2\theta[\pm x,\pm y] - (2J)^{-1} - & |\text{ acquire} \\ & | & | \\ ^1H_X & | \quad \text{selective decoupling for} & | \\ & | \quad \text{alternate transients} & | \end{array} \qquad (20)$$

The method relies on the homonuclear coupling (J) between two adjacent protons in the metabolite, H_A and H_X, e.g. between the lactate CH_3 and CH protons. Single frequency decoupling is applied to H_X for alternate transients which are subtracted.

2. Selective inversion. If binomial water suppression is used, and H_X lies in the unexcited window (as will be common when H_X is a CH proton and H_A are CH_2 or CH_3 protons), the method becomes exactly analogous to the heteronuclear case. Writing the binomial pulses as θ_w, the method becomes

$$\begin{array}{lll} ^1H & \theta_w - \tau - 2\theta_w[\pm x,\pm y] - \tau - \text{acquire} \\ & | \\ ^1H_X & |\ - J^{-1} - 2\Phi_S[x,\bar{0}] \end{array} \qquad (21)$$

$2\Phi_S$ is a chemical shift selective 180° pulse applied just to H_X, and since both H_A and H_X are separately irradiated in the sequence, it functions in the same way as sequence (19). For $2\Phi_S$ to be selective, it will be of tens of milliseconds duration, so τ is set geater than J^{-1} to permit this. Hetherington et al (123) have used this method to detect lactate and alanine in the rat brain postmortem using a surface coil. We have since been thwarted by significant errors arising from intervening fat layers in other applications, but have theoretically proposed that the use of the equivalent sequence

$$\begin{array}{lll} ^1H & \theta_w - \tau - 2\theta_w[\pm x, \pm y] - \tau - | \text{ acquire} \\ & & | \\ ^1H_X & 2\Phi_S[x,\bar{0}] - J^{-1} - | \end{array} \qquad (22)$$

in addition to (21) will eliminate this (128). Recent results appear to confirm this (74). Note that by analogy with sequence (19) , complete localization can be achieved with sequences (21) and (22) using appropriate binomial depth pulses in place of θ_w and by applying the θ and Φ pulses with separate coils. Alternatively the pulsed field gradient methods of section V could be combined with these editing methods.

XI. CONCLUSION

Given the reality of large-bore high field strength magnets, and spectrometers that will deliver any sequence of hard or soft pulses with or without pulsed field gradients, the challenge is to optimize localization, sensitivity and spectral editing for *in vivo* NMR spectroscopy. A plethora of different methods has resulted and there are now real solutions to the problem of sensitive-volume localization, though none are in routine use -- insufficient time has passed. Although we may now have a reasonable idea of the range of possible solutions, no doubt new solutions will be devised for some time to come, and the task of optimizing the present methods for routine application has hardly begun. It is impossible to conclude that one method is best overall -- that conclusion depends on the particular investigation in mind. However, in any one case it is possible to assess the sources of errors and judge whether a localization method is required or sufficient. Perhaps the biggest worry is whether there will be sufficient intrinsic signal-to-noise to permit the routine use of localization procedures. Certainly, the need for maximum sensitivity ensures the future importance of inhomogeneous coils.

REFERENCES

[1]E.A. Shoubridge, R.W. Briggs and G.K. Radda, *FEBS Lett.* **140**, 288 (1982).

[2] J.J.H. Ackerman, J.L. Evelhoch, B.A. Berkowitz and G.M. Kichura, R.K. Devel and K.S. Lown, *J. Magn. Reson.* **56**, 318 (1984).

[3]M.G. Crowley, J.L. Evelhoch and J.J.H. Ackerman, *Proceedings of the Third Annual Meeting of the Society of Magnetic Resonance in Medicine* (New York, August 1984), p.173.

[4]M.R. Bendall and R.E. Gordon, *J. Magn. Reson.* **53**, 365 (1983); M.R. Bendall, U.S. Patent No. 4,486,709 (1984).

[5]M.R. Bendall in *Biomedical Magnetic Resonance* (T.L. James and A.R. Margulis, Eds.), p. 99, Radiology Research and Education Foundation, San Francisco, 1984.

[6]M.R. Bendall and D.T. Pegg, *Magn. Reson. Med.* **2**, 91 (1985).

[7]M.R. Bendall, *J. Magn. Reson.* **59**, 406 (1984).

[8]W.P. Evanochko, T.C. Ng, T.T. Sakai, N.R. Krishna and J.D. Glickson, *Magn. Reson. Med.* **1**, 149 (1984).

[9]D.E. Demco, P. Van Hecke and J.S. Waugh, *J. Magn. Reson.* **16**, 467 (1974).

[10]J.L. Evelhoch and J.J.H. Ackerman, *J. Magn. Reson.* **53**, 52 (1983).
[11]T.C. Ng, J.D. Glickson and M.R. Bendall, *Magn. Reson. Med.* **1**, 450 (1984).
[12]G. Bodenhausen, R. Freeman and D.L. Turner, *J. Magn. Reson.* **27**, 511 (1977).
[13]M.R. Bendall and D.T. Pegg, *J. Magn. Reson.* **63**, 494 (1985).
[14]J.J.H. Ackerman, T.H. Grove, G.C. Wong, D.G. Gadian and G.K. Radda, *Nature (London)* **283**, 167 (1980).
[15]A. Haase, W. Hänicke and J. Frahm, *J. Magn. Reson.* **56**, 401 (1984).
[16]J.L. Evelhoch, M.G. Crowley and J.J.H. Ackerman, *J. Magn. Reson.* **56**, 110 (1984).
[17]M.R. Bendall, J.M. McKendry, I.D. Cresshull and R.J. Ordidge, *J. Magn. Reson.* **60**, 473 (1984).
[18]R.J. Ordidge, unpublished results.
[19]R. Freeman, S.P. Kempsell and M.H. Levitt, *J. Magn. Reson.* **38**, 453 (1980).
[20]R. Tycko, H.M. Cho, E. Schneider and A. Pines, *J. Magn. Reson.* **61**, 90 (1985).
[21]H.P. Hetherington, D. Wishart, S.M. Fitzpatrick, P. Cole and R.G. Shulman, *J. Magn. Reson.*, **66**, 313 (1986).
[22]M.H.. Levitt and R.R. Ernst, *J. Magn. Reson.* **55**, 247 (1983).
[23]H.P. Hetherington and D.L. Rothman, *J. Magn. Reson.*, **65**, 348 (1985).
[24]M.R. Bendall and D.T. Pegg, *J. Magn. Reson.*, **67**, 376 (1986).
[25]M.R. Bendall and D.T. Pegg, unpublished results.
[26]M.S. Silver, R.I. Joseph and D.I. Hoult, *Phys. Rev. A.* **31**, 2753 (1985).
[27]M.R. Bendall, *Bull. Magn. Reson.* **5**, 191 (1983).
[28]M.R. Bendall, *Magn. Reson. Med.*, **1**, 105 (1984).
[29]D.I. Hoult, *J. Magn. Reson.* **35**, 69 (1979).
[30]P.R. Locher, *Phil. Trans. Roy. Soc. London Ser. B.* **289**, 537 (1980).
[31]C. Bauer, R. Freeman, T. Frenkiel, J. Keeler and A.J. Shaka, *J. Magn. Reson.* **58**, 442 (1984).
[32]M.S. Silver, R.I. Joseph and D.I. Hoult, *J. Magn. Reson.* **59**, 347 (1984).
[33]J. Frahm and W. Hänicke, *J. Magn. Reson.* **60**, 320 (1984).
[34]P.A. Bottomley, T.B. Foster and R.D. Darrow, *J. Magn. Reson.* **59**, 338 (1984).
[35]P.A. Bottomley, W.A. Edelstein, T.H. Foster and W.A. Adams, *Proc. Nat. Acad. Sci.*, **82**, 2148 (1985).
[36]R.J. Ordidge, M.R. Bendall, R.E. Gordon and A. Connelly, *Proceedings of the Eleventh Biennial International Conference of Magnetic Resonance in Biological Systems* (Goa, September 1984), p.387.
[37]R.J. Ordidge, A. Connelly and J.A.B. Lohman, *J. Magn. Reson.*, **66**, 283 (1986).
[38]I.R. Young, U.K. Patent application No. 2,122, 753A.
[39]W.P. Aue, S. Müller, T.A. Cross and J. Seelig, *J. Magn. Reson.* **56**, 350 (1984).
[40]S. Müller, W.P. Aue and J. Seelig, *J. Magn. Reson.* **63**, 530 (1985).
[41]H. Post, P. Brünner and D. Ratzel, *Bruker Medizintechnik.*,Karlsruhe FRG, personal communication.
[42]M. Garwood, personal conmunication.
[43]M.R. Bendall in *Magnetic Resonance in Cancer* (P.S. Allen, D.P.J. Boisert and B.C. Lentle, Eds.), p. 159, Pergamon, Toronto, 1986.
[44]A.A. Maudsley, S.K. Hilal, W.H. Perman and H.E. Simon, *J. Magn. Reson.* **51**, 147 (1983).
[45]J.C. Haselgrove, V.H. Subramanian, J.S. Leigh, L. Gyulai and B. Chance, *Science* **220**, 1170 (1983).
[46]R. J. Ordidge, personal communication.
[47]W.A. Edelstein, *Proceedings of the Third Annual Meeting of the Society of Magnetic Resonance in Medicine* (New York, August 1984), p. 202.
[48]D.L. Rothman, personal communication.
[49]H.R. Brooker and T.H. Mareci, *Magn. Reson. Med.*, **1**, 118 (1984).
[50]T.H. Mareci and H.R. Brooker, *J. Magn. Reson.* **57**, 157 (1984).
[51]T.H. Mareci, R.G. Thomas, K.N. Scott and H.R. Brooker, *Proceedings of the Third Annual Meeting of the Society of Magnetic Resonance in Medicine* (New York, August 1984), p.493.
[52]T.H. Mareci, J.T. Mao. K.N. Scott and H.R. Brooker, *Proceedings of the Fourth Annual Meeting of the Society of Magnetic Resonance in Medicine* (London, August 1985), p.1022.
[53]K.N. Scott, H.R. Brooker, J.R. Fitzsimmons, H.F. Bennett and R.C. Mick, *J. Magn. Reson.* **50**, 339 (1982).
[54]K.N. Scott, R.A. Schurehaus, J.R. Fitzsimmons, R.C. Mick, H.F. Bennett and H.R. Brooker, *Magn. Reson. Med.* **1**, 246 (1984).
[55]R.C. Mick, J.R. Fitzsimmons, K.N. Scott and R.A. Schuerhaus, *Magn. Reson. Med.* **1**, 203 (1984).

[56]K.N. Scott in *Biomedical Magnetic Resonance* (T.L. James and A.R. Margulis, Eds) p. 79, Radiology Research and Education Foundation, San Francisco, 1984.

[57]A. Macovski, *Magn. Reson. Med.* **2**, 29 (1985).

[58]I. Shenberg and A. Macovski, *Proceedings of the Fourth Annual Meeting of the Society of Magnetic Resonance in Medicine* (London, August 1985), p. 1056.

[59]D.I. Hoult, *J. Magn. Reson.* **33**, 183 (1979).

[60]S.J. Cox and P. Styles. *J. Magn. Reson.* **40**, 209 (1980).

[61]P.H. Bolton, *J. Magn. Reson.* **63**, 620 (1985).

[62]A. Haase, C. Malloy and G.K. Radda, *J. Magn. Reson.* **55**, 164 (1983).

[63]M. Garwood, T. Schleich, G.B. Matson and G. Acosta, *J. Magn. Reson.* **60**, 268 (1984).

[64]M.R. Bendall, *Chem. Phys. Lett.* **99**, 310 (1984).

[65]M.R. Bendall and W.P. Aue, *J. Magn. Reson.* **54**, 149 (1983).

[66]T.C. Ng and M.R. Bendall, *Magn. Reson. Med.* **1**, 216 (1984).

[67]M.R. Bendall, *Proceedings of the Third Annual Meeting of the Society of Magnetic Resonance in Medicine* (New York, August 1984), p.41.

[68]M.R. Bendall and D.T. Pegg, *J. Magn. Reson.* **68**, 252 (1986).

[69]A.J. Shaka and R. Freeman, *J. Magn. Reson.* **62**, 340 (1985).

[70]A.J. Shaka and R. Freeman, *J. Magn. Reson.* **64**, 145 (1985).

[71]M. Decorps, M. Laval, A. Confort and J.-J. Chaillout, *J. Mag. Reson.* **61**, 418 (1985).

[72]W.M. Chew, M.E. Moseley, M.C. Nishimura and T.L. James, *Proceedings of the Fourth Annual Meeting of the Society of Magnetic Resonance in Medicine* (London, August 1985), p.952.

[73]R. Gonzalez-Mendez, M.E. Moseley, J. Murphy-Boesch, W.M. Chew, L. Litt and T.L. James, *Proceedings of the Fourth Annual Meeting of the Society of Magnetic Resonance in Medicine* (London, August 1985), p.971.

[74]C.C. Hanstock, D.P. Boisvert and M.R. Bendall, unpublished results.

[75]D.G. Gadian, E. Proctor, S.R. Williams, I.J. Cox and R.M. Gardiner, *Proceedings of the Fourth Annual Meeting of the Society of Magnetic Resonance in Medicine* (London, August 1985), p. 785.

[76]M. Decorps, P. Blondet and J.P. Albrand, *Proceedings of the Fourth Meeting of the Society of Magnetic Resonance in Medicine* (London, August 1985), p.779.

[77]A.J. Shaka and R. Freeman, *J. Magn. Reson.* **59**, 169 (1984).

[78]A.J. Shaka, J. Keeler, M.B. Smith and R. Freeman, *J. Magn. Reson.* **61**, 175 (1985).

[79]R. Tycko and A. Pines, *J. Magn, Reson*, **60**, 156 (1984).

[80]M. Garwood, T. Schleich, B.D. Ross, G.B. Matson and W.D. Winters, *J. Magn. Reson.* **65**, 239 (1985).

[81]M. Garwood, T. Schleich, M.R. Bendall and D.T. Pegg, *J. Magn. Reson.*, **65**, 510 (1985).

[82]K.R. Metz and R.W. Briggs, *J. Magn. Reson.* **64**, 172 (1985).

[83]J. Pekar, J.S. Leigh and B. Chance, *J. Magn. Reson.* **64**, 115 (1985).

[84]J. Pekar, P.F. Renshaw and J.S. Leigh, *Proceedings of the Fourth Annual Meeting of the Society of Magnetic Resonance in Medicine* (London, August 1985), p. 176.

[85]J. Pekar and J.S. Leigh, *Proceedings of the Fourth Annual Meeting of the Society of Magnetic Resonance in Medicine* (London, August 1985), P.178.

[86]G.K. Radda, *Proceedings of the Third Annual Meeting of the Society of Magnetic Resonance in Medicine* (New York, August 1984), p. 605.

[87]D. De Klerk, *The Construction of High-field Electromagnets* p.115, Newport Instruments Ltd,, Newport Pagnell, Bucks, 1965.

[88]M.R. Bendall, A. Connelly and J.M. McKendry, *Magn. Reson. Med.*, **3**, 157 (1986).

[89]P. Styles, personal communication.

[90]P. Styles, M.B. Smith, R.W. Briggs and G.K. Radda, *J. Magn. Reson.* **62**, 397 (1985).

[91]A. Haase, *J. Magn. Reson.* **61**, 130 (1985).

[92]L.K. Hedges and D.I. Hoult, *Proceedings of the Fourth Annual Meeting of the Society of Magnetic Resonance in Medicine* (London August 1985), p.1096.

[93]P. Styles, C.A. Scott and G.K. Radda, *Magn. Reson. Med.* **2**, 402 (1985).

[94]M. G. Crawley, J. L. Evelhoch and J.J.H. Ackerman, *J. Magn. Reson.* **64**, 20 (1985).

[95]J. Field, W.M. Brooks, J.M. Bulsing, M.G. Irving and D.M. Doddrell *J. Magn. Reson.* **63**, 612 (1985).

[96]R.S. Balaban, D.G. Gadian and G.K. Radda, *Kidney*

Int. **20**, 575 (1981).

[97]G.D. Clarke and R.L. Nunnally, *Proceedings of the Third Annual Meeting of the Society of Magnetic Resonance in Medicine* (New York, August 1984), p.161.

[98]W.G. Holcomb and J.C. Gore, *Proceedings of the Third Annual Meeting of the Society of Magnetic Resonance in Medicine* (New York, August 1984), p. 333.

[99]M.S. Roos, A. Hasenfeld, M.R. Bendall, R.H. Huesman and T.F. Budinger, *Proceedings of the Third Annual Meeting of the Society of Magnetic Resonance in Medicine* (New York, August 1984), p. 632.

[100]A. Jesmanowicz, T.M. Grist, W. Francisz and J.S. Hyde, *Proceedings of the Fourth Annual Meeting of the Society of Magnetic Resonance in Medicine* (London, August 1985), p.489.

[101]M.R. Bendall and J.M. McKendry, European patent application No. 85305397.3.

[102]M.R. Bendall and D.T. Pegg, *J. Magn. Reson.* **57**, 337 (1984).

[103]M.R. Bendall and D.T. Pegg, *Magn. Reson. Med.* **2**, 298 (1985).

[104]D.T. Pegg, D.M. Doddrell and M.R. Bendall, *J. Chem Phys.* **77**, 2745 (1982).

[105]D.T. Pegg and M.R. Bendall, *Magn. Reson. Med.* **2**, 453 (1985).

[106]M.R. Bendall and D.T. Pegg, *J. Magn. Reson.* **53**, 272 (1983).

[107]M.R. Bendall, J.A. den Hollander, F. Arias-Mendoza, D.L. Rothman, K.L. Behar and R.G. Shulman, *Magn. Reson. Med.* **2**, 56 (1985).

[108]D.T. Pegg and M.R. Bendall, *J. Magn. Reson.*, **63**, 556 (1985).

[109]M.R. Bendall, D.T. Degg, D.M. Doddrell and J. Field, *J. Magn.Reson.* **51**, 520 (1983).

[110]D.T. Pegg and M.R. Bendall, *J. Magn. Reson.* **55**, 114 (1983).

[111]W.P. Aue, S. Müller and J. Seelig, *J. Magn. Reson.* **61**, 392 (1985).

[112]D.J. Cookson and B.E. Smith, *Org. Magn. Reson.* **16**,111 (1981).

[113]D.W. Brown, T.T. Nakashima and D.L. Rabenstein, *J. Magn. Reson.* **45**, 302 (1981).

[114]M.R. Bendall, D.T. Pegg, D.M. Doddrell and D.H. Williams, *J. Org. Chem.* **47**, 3021 (1982).

[115]D.L. Rothman, K.L. Behar. H.P. Hetherington, J.A. den Hollander, M.R. Bendall, O.A.C. Petroff and R.G. Shulman, *Proc. Nat. Acad. Sci. USA*, **82**, 1633 (1985).

[116]M.R. Bendall. D.T. Pegg, D.M. Doddrell and J. Field, *J. Am. Chem. Soc.* **103**, 934 (1981).

[117]R. Freeman, T.H. Mareci and G.A. Morris, *J. Magn. Reson,* **42**, 341 (1981).

[118]S.R. Williams. D.G. Gadian, E. Proctor, D.B. Sprague, D. F. Talbot, I.R. Young and F.F. Brown, *J. Magn. Reson.* **63**, 406 (1985).

[119]V. Sklenár and Z. Starcuk, *J. Magn. Res.* **50**, 495 (1982).

[120]P.J. Hore, *J. Magn. Reson.* **55**, 283 (1983).

[121]Z. Starcuk and V. Sklenár, *J. Magn. Reson.* **61**, 567 (1985), and refs. therein.

[122]K.M. Brindle. R. Porteous and I.D. Campbell, *J. Magn Reson.* **56**, 543 (1984).

[123]H.P. Hetherington, M.J. Avison and R.G. Shulman, *Proc. Nat. Acad. Sci., U.S.A.* **82**, 3115 (1985).

[124]M.R. Bendall and H.P. Hetherington, unpublished results.

[125]D.L. Rothman, F. Arias-Mendoza, G.I. Shulman and R.G. Shulman, *J. Magn. Reson.* **60**, 430 (1984).

[126]I.D. Campbell and C.M. Dobson, *J.C.S. Chem. Comm.*, 751 (1975).

[127]D.L. Rothman, K.L. Behar, H.P. Hetherington and R.G. Shulman, *Proc. Nat. Acad. Sci., U.S.A.* **81**, 6330 (1984).

[128]H.P. Hetherington, D.L. Rothman and M.R. Bendall, unpublished results.